Regulation of ubiquitin ligase dynamics by the nucleolus

Karim Mekhail,[1] Mireille Khacho,[1] Amanda Carrigan,[2] Robert R.J. Hache,[2] Lakshman Gunaratnam,[1] and Stephen Lee[1]

[1]Department of Cellular and Molecular Medicine, Faculty of Medicine, University of Ottawa, Ottawa, Ontario K1H 8M5, Canada
[2]Ottawa Health Research Institute, University of Ottawa, Ottawa, Ontario K1Y 4E9, Canada

Cellular pathways relay information through dynamic protein interactions. We have assessed the kinetic properties of the murine double minute protein (MDM2) and von Hippel-Lindau (VHL) ubiquitin ligases in living cells under physiological conditions that alter the stability of their respective p53 and hypoxia-inducible factor substrates. Photobleaching experiments reveal that MDM2 and VHL are highly mobile proteins in settings where their substrates are efficiently degraded. The nucleolar architecture converts MDM2 and VHL to a static state in response to regulatory cues that are associated with substrate stability. After signal termination, the nucleolus is able to rapidly release these proteins from static detention, thereby restoring their high mobility profiles. A protein surface region of VHL's β-sheet domain was identified as a discrete [H+]-responsive nucleolar detention signal that targets the VHL/Cullin-2 ubiquitin ligase complex to nucleoli in response to physiological fluctuations in environmental pH. Data shown here provide the first evidence that cells have evolved a mechanism to regulate molecular networks by reversibly switching proteins between a mobile and static state.

Introduction

Conjugation of ubiquitin (ubiquitylation) to proteins destines them for very different fates in the cell (Weissman, 2001; Muratani and Tansey, 2003; Ciechanover, 2005). Although targeting proteins for degradation via the 26S proteasome is the best-studied role of ubiquitylation, this modification is integral to several biochemical pathways including receptor internalization (Terrell et al., 1998), chromatin maintenance (Muratani and Tansey, 2003) and DNA repair (Russell et al., 1999; Gillette et al., 2001). The ubiquitin system is sustained by the interaction of multiple dynamic molecular networks that begin with the loading of ubiquitin onto an ubiquitin-activating enzyme (E1). The ubiquitin moiety is then transferred to a ubiquitin-conjugating enzyme (E2), and finally, a ubiquitin protein ligase (E3) catalyses the transfer of ubiquitin from E2 to the lysine residue of a specific substrate, thereby altering its cellular fate.

There are many more E3s in the cell than there are E1s and E2s combined, and it is thought that E3s determine the specificity of substrate recognition within the ubiquitin system. The function of a ubiquitin ligase can be regulated by controlling the ligase or its substrate at various levels such as post-translational modifications, interactions with regulatory factors, or subcellular localization (Petroski and Deshaies, 2005).

The complexity of E3 regulatory mechanisms is well demonstrated by the mechanisms controlling the degradation of the p53 tumor suppressor protein (Michael and Oren, 2003). The murine double minute protein MDM2 ubiquitin ligase targets p53 for ubiquitylation in the nucleus followed by nuclear export and degradation by cytoplasmic 26S proteasome (Momand et al., 1992; Oliner et al., 1993; Freedman and Levine, 1998; Roth et al., 1998). Various signals can alter the function of MDM2 within this setting. DNA damage rapidly activates the ataxia telangiectasia mutated protein, which phosphorylates MDM2 to prevent the ubiquitylation of p53 (Appella and Anderson, 2001). Replicative senescence induces the tumor suppressor ARF to bind MDM2 and inactivate it by both immediately reducing its ability to recognize p53 in the nucleoplasm (Llanos et al., 2001) and translocating MDM2 to the nucleolus (Tao and Levine, 1999; Weber et al., 1999), a major nuclear compartment (Carmo-Fonseca et al., 2000). Similarly, perturbations to ribosomal biogenesis induce the ribosomal protein L11 to bind MDM2 and inhibit its function by relocating it to the nucleolus (Lohrum et al., 2003).

Correspondence to Stephen Lee: slee@uottawa.ca

Abbreviations used in this paper: ActD, actinomycin D; AP, acidification-permissive; B23, rRNA processing-factor nucleophosmin; FIB, rRNA processing factor fibrillarin; FLIP, fluorescence loss in photobleaching; HIF, hypoxia-inducible factor; iFRAP, inverse FRAP; MDM2, murine double minute protein; NES, nuclear export sequence; NoDS^{H+}, [H$^+$]-responsive nucleolar detention signal; NoLS, nucleolar localization sequence; NoRS, nucleolar retention sequence; PEG, polyethylene glycol; RS, ribosomal stress; SD media, standard media; VHL, von Hippel-Lindau.

The online version of this article contains supplemental material.

The Journal of Cell Biology, Vol. 170, No. 5, August 29, 2005 733–744
http://www.jcb.org/cgi/doi/10.1083/jcb.200506030

Functional regulation of E3s by the nucleolus has also been observed in the von Hippel-Lindau (VHL) tumor suppressor/hypoxia-inducible factor (HIF) system (for review see Kaelin, 2002; Mekhail et al., 2004a). HIF activates an array of genes that mediate cellular response to low oxygen availability (Semenza, 2000). In the presence of oxygen, the α subunit of HIF (HIFα) is post-translationally modified by enzymes known as prolyl hydroxylases (PHDs). This allows the VHL tumor suppressor, the particle recognition motif of an elongin C/Cullin-2 ubiquitin ligase, to recognize HIFα and target it for nuclear ubiquitylation. VHL-mediated shuttling of HIFα to the cytoplasm then results in its destruction by the 26S proteasome (Lee et al., 1999; Groulx and Lee, 2002) in a manner reminiscent of the MDM2/p53 system. Several physiological cues can modulate the function of VHL within this setting. PHDs require molecular oxygen and hypoxia prevents hydroxylation of HIF, allowing it to evade recognition by VHL and degradation. In addition, we previously reported that a decrease in environmental pH triggers the relocation of VHL to the nucleolus, neutralizing its ability to degrade nuclear HIF even in the presence of oxygen (Mekhail et al., 2004a,b).

The nucleolus has traditionally been viewed as a factory for the production of ribosomes (Lam et al., 2005). More recently, this nuclear compartment has been linked to numerous cellular activities including cell cycle control (Shou et al., 1999, 2001; Visintin et al., 1999; Azzam et al., 2004), DNA damage repair (van den Boom et al., 2004), and tRNA processing (Paushkin et al., 2004). Although the nucleolus has a distinct set of "resident" proteins, it is now clear that these proteins are in continuous flux between the nucleolus and other cellular compartments (Dundr et al., 2000, 2002; Phair and Misteli, 2000; Chen and Huang, 2001; Misteli, 2001; Carmo-Fonseca, 2002; Andersen et al., 2005; Tsai and McKay, 2005). This dynamic nature is facilitated by a fundamental characteristic of nuclear compartments; that is the lack of a delineating membrane. For example, thousands of molecules of the rRNA processing factor fibrillarin (FIB), which displays steady-state nucleolar localization, exit the nucleolus each second (Phair and Misteli, 2000). The highly dynamic properties of proteins in the nucleus follow a stochastic model of high molecular mobility to ensure efficient functional interactions (Misteli, 2001). An advantage of such probabilistic movement is the ability to achieve rapid responses to signaling cues. For example, a slight increase in the quantity of a modified protein results in a relatively high probability of encountering its target. As mentioned above, resident nucleolar proteins are dynamic molecules that can functionally engage in subcellular trafficking between the nucleolus and other cellular compartments. Therefore, it remains unclear how the highly dynamic nucleolus inactivates the function of E3 enzymes, as these macromolecules would be predicted to retain their dynamic nature and maintain functional molecular interactions.

Here, we report the unexpected observation that the nucleolar architecture is able to reversibly capture and alter the dynamic properties of ubiquitin ligases. We show that VHL and MDM2 are highly mobile proteins that can be statically detained by the nucleolus to prevent functionally required molec-

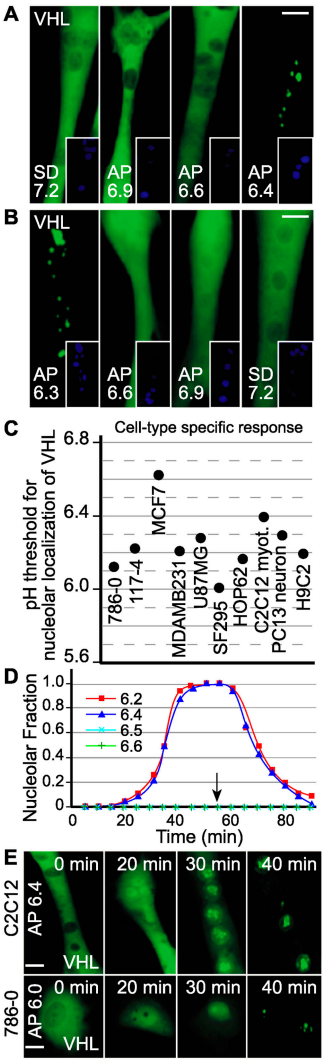

Figure 1. **pH-dependent kinetics of VHL subcellular trafficking.** (A) C2C12-differentiated myotubes were cultured in standard (SD) media and infected to express adenovirus-introduced VHL-GFP. Cells were replenished with either fresh SD media (pH 7.2) or different AP media (initial pH 7.2) that allow maximal extracellular acidification to pH 6.9, 6.6, 6.4, 6.2, or 6.0 (see Materials and methods). Cells were transferred to hypoxia (1% O_2) for 18 h. VHL redistributed to nucleoli only in conditions of pH 6.4 or lower (images of pH 6.2 and 6.0 are not depicted). Extracellular pH is indicated on each panel. Insets show Hoechst staining of DNA. Bars (A, B, and E), 10 μm. (B) After localization of VHL-GFP to the nucleolus, myotubes were replenished with AP media previously maximally acidified to indicated pH levels, or with fresh SD media. VHL reverted to nucleo-cytoplasmic distribution only when the pH of the media was higher than 6.4. (C) Different cell types were treated as in A and B to identify the pH thresholds required for nucleolar targeting of VHL ($n = 40$ for each tested pH value). (D) Kinetics of VHL nucleolar localization in acidosis and release after neutralization in differentiated myotubes. Cells were exposed to different AP media as in A to induce VHL nucleolar redistribution, and all media were neutralized to pH 7.2 by addition of NaOH (arrow). Time zero indicates time at which the pH of AP media reached 6.4. For the 6.5 and 6.7 sets, time zero is matched to that of the pH 6.4 set. (E) Cells were incubated in AP media (initial pH 7.2) that blocks acidification beyond pH 6.0. After reaching the acidification level matching the pH threshold required to trigger nucleolar targeting of any given cell-type (time zero), the localization of VHL-GFP was monitored over time. Upon reaching the pH threshold, VHL shifts from mainly cytoplasmic to mainly nucleoplasmic before triggering nucleolar localization.

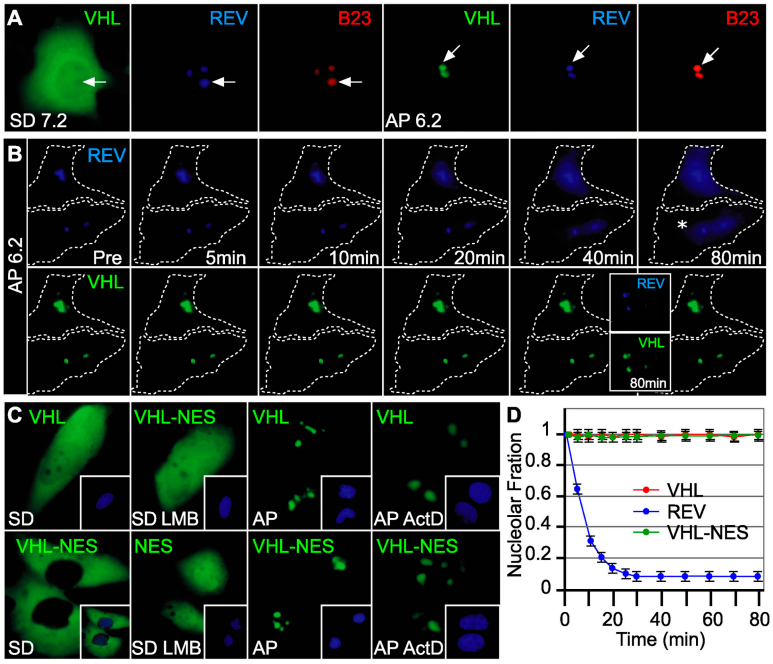

Figure 2. **Kinetics of nucleolar VHL and REV.** (A and B) MCF7 cells cotransfected to express VHL-GFP and REV-BFP were incubated in hypoxia in SD or AP conditions. After localization of VHL-GFP to the nucleolus, cells were either fixed and immunostained for nucleolar B23 (A) or treated with 10 μg/ml ActD and monitored over time (B). Arrows in A indicate the same position in the cell and dashed cellular outlines are shown in B. Insets in B show a time-matched set that was not treated with ActD. (C and D) VHL-GFP-NES fusion protein is not released from nucleoli after ActD treatment. MCF7 cells were transfected to express VHL-GFP, VHL-GFP-NES, or GFP-NES alone and transferred to hypoxia in SD or AP media. Shown are images 50 min after AP media reached the pH 6.5 threshold. Where indicated, leptomycin B (LMB) was added when AP media reached pH 6.65 (usually 30–40 min) before pH 6.5 time point. Insets in C show Hoechst staining of DNA. (D) Ratiometric fluorescence measurements of hypoxic-acidotic cells initially displaying nucleolar REV-BFP, VHL-GFP, and VHL-GFP-NES after ActD treatment.

ular interactions in response to physiological cues. Based on these data, we suggest that cells have evolved a mechanism to regulate the function of proteins by reversibly switching them between mobile and static states.

Results

[H+]-regulated kinetics of VHL subcellular trafficking

Ischemic tissues or hypoxic cells normally acidify their extracellular milieu as a physiological consequence of anaerobic glycolysis. This is best exemplified by muscle fatigue, in which myotubes produce lactic acid after exposure to hypoxia. Study of the ubiquitin ligase component VHL within this setting revealed its functional regulation by changes in environmental H^+ concentrations (Mekhail et al., 2004a). VHL engages in nuclear/cytoplasmic trafficking in neutral conditions but accumulates in the nucleolus upon a decrease in extracellular pH, a process that results in stabilization of its substrate HIF. Differentiated myotubes can be incubated in standard (SD) media, which prevents fluctuations in pH, or in acidification-permissive (AP) media, which is prepared to enable hypoxic cells to acidify their extracellular milieu to varying degrees (see Materials and methods) (Mekhail et al., 2004a). VHL-GFP is observed in its typical diffuse nuclear cytoplasmic distribution under neutral pH conditions, independent of oxygen tension (Fig. 1 A, left; Mekhail et al., 2004a). A rapid redistribution of VHL-GFP to nucleoli was observed only when hypoxic myotubes were incubated in AP media that allow the myotubes to acidify their environment to pH 6.40 or lower (Fig. 1, A and D; see Fig. S1, A and B, for cell viability controls, available at http://www.jcb.org/cgi/content/full/jcb.200506030/DC1), indicating the existence of a pH threshold required for triggering nucleolar localization of VHL. The threshold displayed cell type–specific differences within the 6.60–5.80 pH range (Fig. 1 C; Fig. S2). VHL efficiently reverted to a diffuse nuclear-cytoplasmic localization under hypoxic conditions only when cells were replenished with media at values higher than the pH threshold required to trigger nucleolar localization (Fig. 1, B–D). Closer examination of this system reveals that the relocation of VHL to the nucleolus is a two-step process, where the protein displays an initial shift from mainly cytoplasmic to mainly nucleoplasmic localization before initiating any detectable targeting to the nucleolus, in all tested cell lines (Fig. 1 E; Fig. S1, C and D). These data suggest that the subcellular trafficking dynamics of VHL are regulated by a multilayered cellular mechanism that gauges environmental hydrogen ion concentrations.

Different kinetics of nucleolar VHL and resident nucleolar proteins after transcriptional inhibition

Due to the role of the nucleolus in ribosomal biogenesis, perturbations to transcription, such as by treatment with low levels of actinomycin D (ActD), alter the trafficking properties of steady-state nucleolar proteins between the nucleolus and the nucleoplasm (Chen and Huang, 2001; Andersen et al., 2005). For example, the human immunodeficiency virus (HIV) mRNA exporter REV is a dynamic nucleolar protein that redistributes to the nucleoplasm and cytoplasm after transcriptional inhibition under both neutral (unpublished data; Stauber et al., 1995; Daelemans et al., 2005) and acidic (Fig. 2 A; Fig. 2 B, top) conditions. In contrast, the nucleolar localization of VHL in acidosis persisted in the absence of transcription (Fig. 2 B, bottom). Similar results were obtained in experiments using VHL-BFP and REV-GFP (unpublished data). The ability of REV to rapidly alter its steady-state distribution under these conditions is greatly enhanced by its strong nuclear export sequence (NES). We therefore tested whether fusion of this NES

to VHL would enable it to release from nucleoli of acidotic cells after transcriptional inhibition. VHL-GFP-NES fusion localized almost exclusively to the cytoplasm under neutral conditions but was restricted to nucleoli at steady-state under acidosis (Fig. 2 C). ActD treatment failed to release the VHL-GFP-NES fusion protein from nucleoli (Fig. 2, C and D), suggesting that the subcellular trafficking dynamics of VHL in the nucleolus significantly differ from the dynamics of resident nucleolar proteins.

Physiological regulation of VHL ubiquitin ligase dynamics by the nucleolus

We therefore used FRAP to assess how the nucleolus affects the dynamic properties of GFP-tagged VHL in living cells (Lippincott-Schwartz et al., 2003). Specific cellular regions expressing fusion proteins were bleached with the use of a laser pulse that irreversibly quenches the GFP signal, and the recovery of signal in the bleached area was recorded by time-lapse confocal microscopy. The kinetics and extent of recovery of fluorescence in a cellular region after bleaching are reflective of the dynamics of the studied fluorescent chimeras.

Cells cultured under standard neutral conditions displayed an essentially complete recovery of VHL-GFP fluorescence within seconds of bleaching nucleoplasmic (Fig. 3, A and G) or cytoplasmic (see Fig. 7 D) regions. We first assessed the capacity of the nucleolus to sustain dynamic shuttling under acidosis by monitoring resident nucleolar proteins, such as the rRNA-processing factors fibrillarin (FIB) and nucleophosmin (NPM or B23), as well as the RNA polymerase I preinitation factor upstream binding factor 1 (UBF1). Acidosis did not alter the steady-state distribution of any of the studied resident nucleolar proteins (Fig. 3, D and E) compared with neutral conditions. In addition, these proteins displayed a rapid pH-independent recovery of fluorescence after bleaching of a single nucleolus within cells with multiple nucleoli (Fig. 3, C and F), indicating dynamic protein shuttling between nucleoli of acidotic cells. In contrast, nucleolar VHL failed to display recovery of fluorescence under the same culture and bleaching parameters (Fig. 3, B and G), suggesting that acidosis alters the mobility profile of VHL. Similar to previous reports, reduction of the temperature from 37 to 22°C did not have any significant effect on the kinetics or extent of recovery of any of the tested proteins in the nucleus or cytoplasm (unpublished data; see Phair and Misteli, 2000). These data suggest that the redistribution of VHL to the nucleolus in response to increases in extracellular hydrogen ion concentrations may alter its general dynamic characteristics in the cell.

The dynamics of VHL were next analyzed by fluorescence loss in photobleaching (FLIP) experiments (Lippincott-Schwartz et al., 2003). In FLIP, a living cell is repeatedly hit with a laser beam in the same region. Loss of fluorescence in an area outside the bleached spot is reflective of protein mobility between that area and the bleached spot. A rapid loss of VHL-GFP fluorescence was observed in essentially the whole nucleus after repetitive bleaching of a small nucleoplasmic region in cells incubated under neutral conditions (Fig. 4 A). Studies presented further in this report (Fig. S3, available at

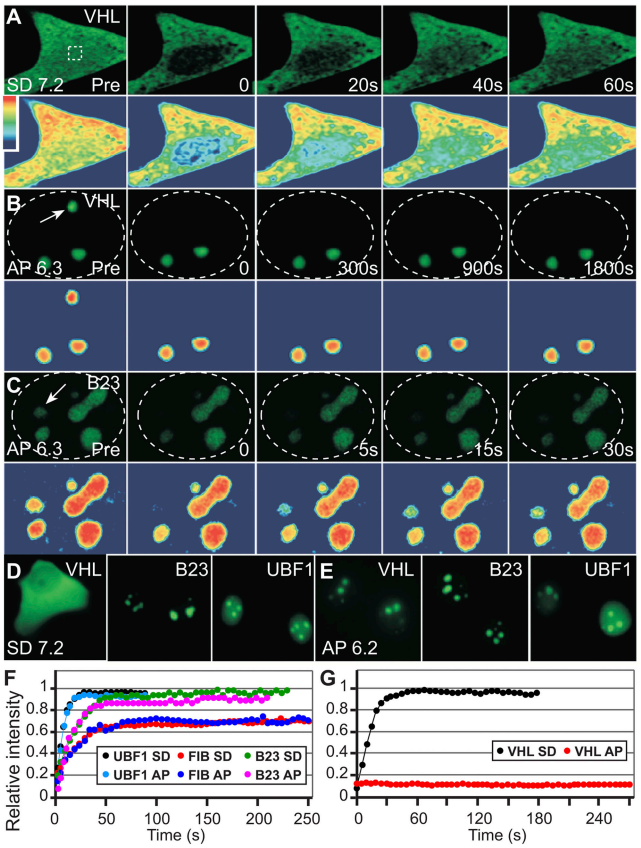

Figure 3. **FRAP analysis reveals that VHL does not shuttle between nucleoli in acidosis.** MCF7 cells transiently transfected to express low levels of VHL-GFP, B23-GFP, FIB-GFP, or UBF1-GFP were incubated in hypoxia under SD or AP conditions. (A–C) Cells were imaged before and after bleaching of indicated nucleoplasmic regions (dashed square) or specific nucleoli (arrows) within nuclei (dashed circles). Post-bleach time is indicated in seconds. Areas of interest are shown as pseudocolored panels to better illustrate minimal changes in fluorescence. (D and E) Steady-state localization of GFP-tagged proteins after incubation in SD or AP media under hypoxia. (F and G) Quantitation of recovery kinetics. Fluorescence intensity in the bleached region was measured and expressed as relative recovery (see Materials and methods). For quantitation, at least 10 cells were analyzed for each result.

http://www.jcb.org/cgi/content/full/jcb.200506030/DC1) will study the nuclear-cytoplasmic trafficking properties of VHL. These observations indicate that VHL participates in dynamic molecular networks.

Next, cells were transfected to express low levels of VHL-GFP to allow for a complete redistribution of the protein chimera to the nucleolus after acidification in hypoxia (Fig. 4 B, first panel; see Mekhail et al., 2004a). Under these conditions, VHL-GFP fluorescence in the nucleolus was unaffected by repetitive bleaching of a nucleoplasmic (Fig. 4, B and F) or cytoplasmic (unpublished data) region. In stark contrast, resident nucleolar proteins rapidly dissociate from the nucleolus in hypoxic-acidotic cells (Fig. 4, C and F). We next examined whether interaction with the nucleolar architecture is required for acidosis-mediated modification of VHL dynamics. Cells were thus transfected to express higher levels of VHL-GFP, saturating nucleolar binding sites and preventing the full redistribution of the fluorescent protein chimera to the nucleolus

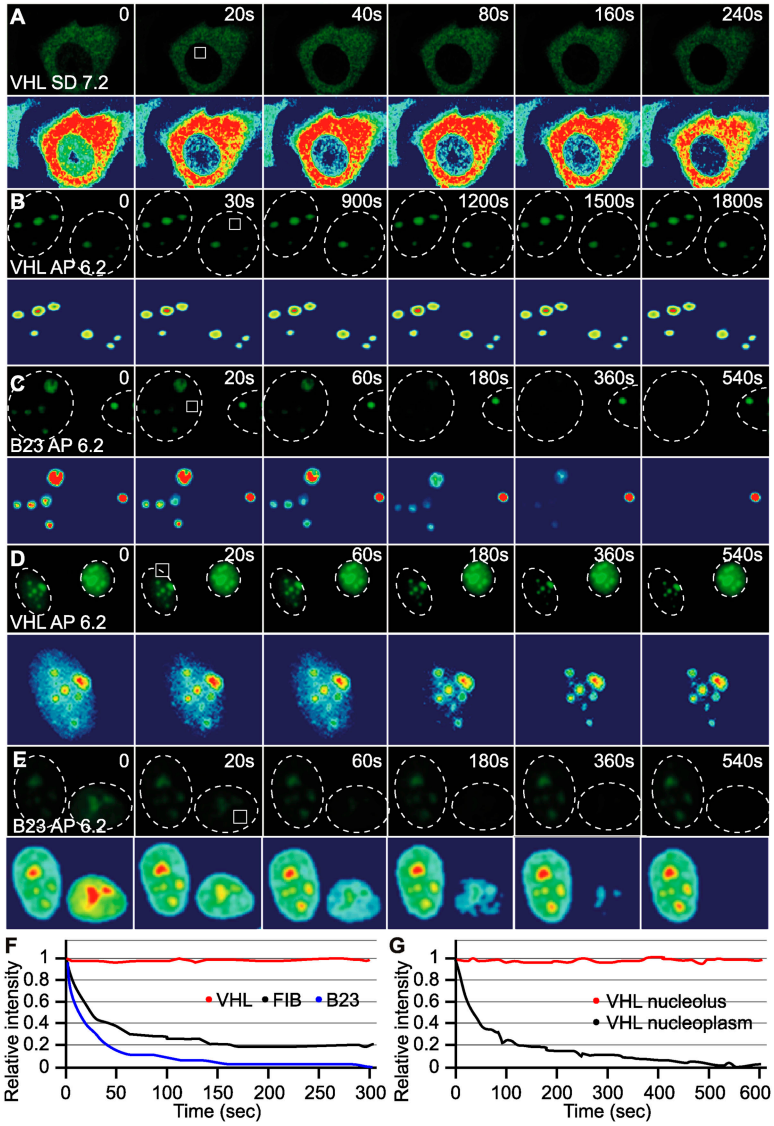

Figure 4. **FLIP analysis reveals that nucleolar VHL does not traffic between the nucleolus and nucleoplasm in acidosis.** MCF7 cells transiently transfected to express low (A–C, and F) or high (D, E, and G) levels of VHL-GFP or B23-GFP were incubated in hypoxia under SD or AP conditions. At time points matching the relocation of VHL-GFP (low levels set) to nucleoli, all cells were submitted to a FLIP analysis where nucleoplasmic regions (white squares) within specific nuclei (dashed circles) were repeatedly bleached. Cells were imaged between pulses. (F and G) Corresponding kinetics of loss of fluorescence.

after acidification in hypoxia (Fig. 4 D, first panel). This establishes two different protein pools in the cell—nucleoplasmic and nucleolar. Although repetitive bleaching of a nuclear region in these cells resulted in complete loss of nucleoplasmic fluorescence, nucleolar VHL-GFP signal remained constant over the course of the experiment (Fig. 4, D, E, and G). No significant bleaching was observed in neighboring nuclei in all of the experiments. Similar to nuclear VHL-GFP under neutral conditions, the nucleoplasmic pool of VHL-GFP in acidosis was able to engage in nuclear export as revealed by inverse FRAP (iFRAP) analysis of living cells (Lippincott-Schwartz et al., 2003), thereby indicating that this nucleoplasmic pool retains functional interactions with the nucleopore architecture in acidosis (Fig. S3). These data indicate that the interaction of VHL with the nucleolar architecture is required for acidosis-mediated modification of VHL protein dynamics.

We next studied VHL dynamics using polykaryon fusion assays, which provide an alternative approach to photobleaching in assessing changes in subcellular trafficking of proteins (Walther et al., 2003). Cells expressing VHL-GFP were fused in a standard polyethylene glycol (PEG) fusion assay. VHL remains nuclear-cytoplasmic in polykaryonic cells (Fig. 5 A, a and b; Lee et al., 1999). Transfer to hypoxia resulted in acidification of the media and VHL-GFP displayed its typical two-step localization process to the nucleolus (Fig. 5 A, c–g). It is important to note that nucleolar VHL signal was equally distributed between the nuclei of a polykaryonic cell (Fig. 5 A), indicating that VHL-GFP displays no preference for the nucleoli of one nucleus over another. Next, we cocultured VHL-GFP–expressing and nonexpressing cells under standard conditions, then transferred them to hypoxia in AP media. After the redistribution of VHL-GFP to nucleoli, cells were rapidly fused and replenished with their own acidified AP media. This process yielded a significant number of polykaryonic cells where the fluorescence observed in the cell is only associated with nucleoli of only one or two nuclei, whereas other nuclei displayed no fluorescence (Fig. 5 B). VHL-GFP failed to exhibit any change in localization up to 3 h after fusion. In contrast, under the same conditions B23-GFP (Fig. 5 C) and REV-GFP (unpublished data) redistributed from the nucleoli of a single cell to the nucleo-cytoplasm and nucleoli of the acceptor

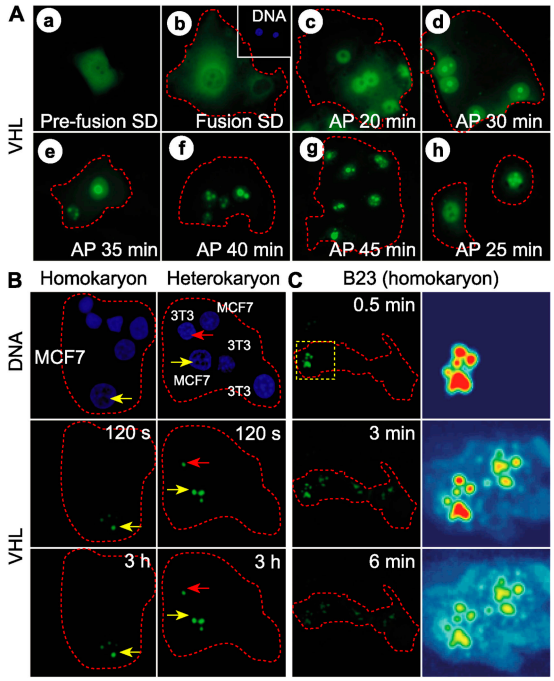

Figure 5. **Long-term detention of VHL within the nucleolar space revealed by the inability of VHL to release from nucleoli in a polykaryon fusion assay.** (A) MCF7 cells transiently expressing VHL-GFP were fused in a standard PEG fusion assay and incubated in SD media for 30 min (b). Inset shows Hoechst staining of DNA. Cells were replenished with AP media and transferred to hypoxia. VHL-GFP localization was monitored after reaching the pH 6.5 threshold (c–g). Nuclei within a polykaryonic cell were always synchronized in the rates of nucleolar appearance of VHL-GFP. This is not necessarily the case for monokaryonic cells in close proximity under AP conditions (h). (B) Unaltered MCF7 cells were cocultured under standard conditions with either MCF7 (homokaryon assay) or NIH 3T3 (heterokaryon assay) cells transfected to transiently express VHL-GFP. Cells were then transferred to hypoxia in AP media. After nucleolar localization of VHL-GFP, cells were fused and monitored by time-lapse microscopy. Hoechst staining of DNA was used to identify donor and acceptor cells. Arrows indicate the same position in the cell. (C) Unaltered MCF7 cells were cocultured under standard conditions with MCF7 cells transfected to transiently express B23-GFP. Cells were cultured in AP media, fused and monitored as in B. Pseudocolored zooms of area indicated by dashed square are shown.

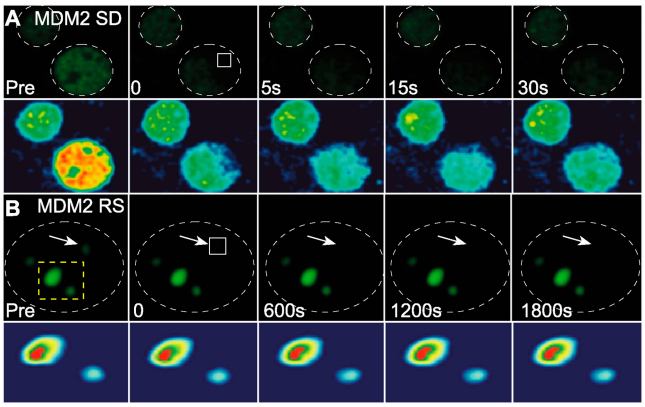

Figure 6. **FRAP analysis reveals that the redistribution of MDM2 from nucleoplasm to nucleoli in response to perturbations in ribosomal biogenesis alters general MDM2 dynamic state.** MCF7 cells transfected to express low levels of MDM2-GFP were cultured either under standard conditions (A), or ribosomal stress (RS) (B) induced by ActD treatment (see Lohrum et al., 2003 and Materials and methods). Cells were submitted to FRAP analysis as described for VHL in Fig. 3 by bleaching the indicated nucleoplasmic regions (white squares) or specific nucleoli (arrows) within specific nuclei (dashed circles). Pseudocolored zoom of area indicated by dashed rectangle is shown in B.

(nontransfected) cells of polykaryons. In addition to bleaching experiments, results from the fusion assays reveal a role for the nucleolus in regulating the subcellular dynamic profile of the VHL tumor suppressor.

Static detention of MDM2 and VHL ubiquitin ligase by the nucleolus

MDM2 displays a diffuse nuclear localization under standard culture conditions. FRAP and FLIP experiments revealed that MDM2 is a highly dynamic protein within this setting (Fig. 6 A; Fig. S4 A, available at http://www.jcb.org/cgi/content/full/jcb.200506030/DC1). MDM2 localizes to the nucleolus in response to perturbations in ribosomal biogenesis after treatment with low levels of ActD that inhibit RNA polymerase I (Fig. 6 B; Fig. S4 B; Lohrum et al., 2003). MDM2 is unable to target p53 for degradation under these conditions. We therefore assessed the dynamics of MDM2 after relocation to the nucleolus. When nucleolar, the dynamic profile of MDM2 significantly changed as GFP fluorescence did not exhibit any recovery/redistribution in FRAP experiments after bleaching of the nucleolus (Fig. 6 B) or loss in FLIP experiments after repetitive bleaching of a nucleoplasmic (Fig. S4 B) or cytoplasmic (unpublished data) region. Similar to VHL (Fig. 4, D and G), the interaction of MDM2 with the nucleolar architecture is required for modification of its trafficking dynamics as evidenced by the quick recovery of MDM2 in the nucleoplasm of transcriptionally inhibited cells expressing high levels of the protein in FRAP (Fig. 7 A). We next evaluated the dynamics of VHL and MDM2 ligases within the nucleolar space. VHL and MDM2 did not exhibit any fluorescence recovery after bleaching of an area within the nucleolus (Fig. 7, A and C). In contrast, B23 remained localized to nucleoli at steady-state within our experimental settings (SD, AP, and RS), retaining its highly mobile properties, though prolonged incubation with ActD resulted in B23 accumulating in the nucleoplasm (Fig. 7 B; unpublished data). Upon photobleaching, a border is created between the bleached area and the gradient of concentration established by the remaining fluorescent molecules (Fig. 7 C). For moving proteins, this border changes its shape as well as its position within the field of vision over time. Statically detained cellular components do not exhibit significant changes in these variables. We therefore compared the characteristics of borders of concentration gradients established by bleaching fluorescently labeled proteins when localized to different regions of the cell. Although analysis of concentration gradient borders in the nucleoplasm and cytoplasm revealed a highly dynamic profile of protein mobility, borders established within the nucleolar space neither changed in shape nor moved within the field of vision for up to 2 h after bleaching (Fig. 7, C–F; unpublished data). A similar static protein profile was observed for MDM2 in the nucleolus (unpublished data). These findings suggest that VHL and MDM2 are targeted for static detention in the nucleolus in response to physiological cues.

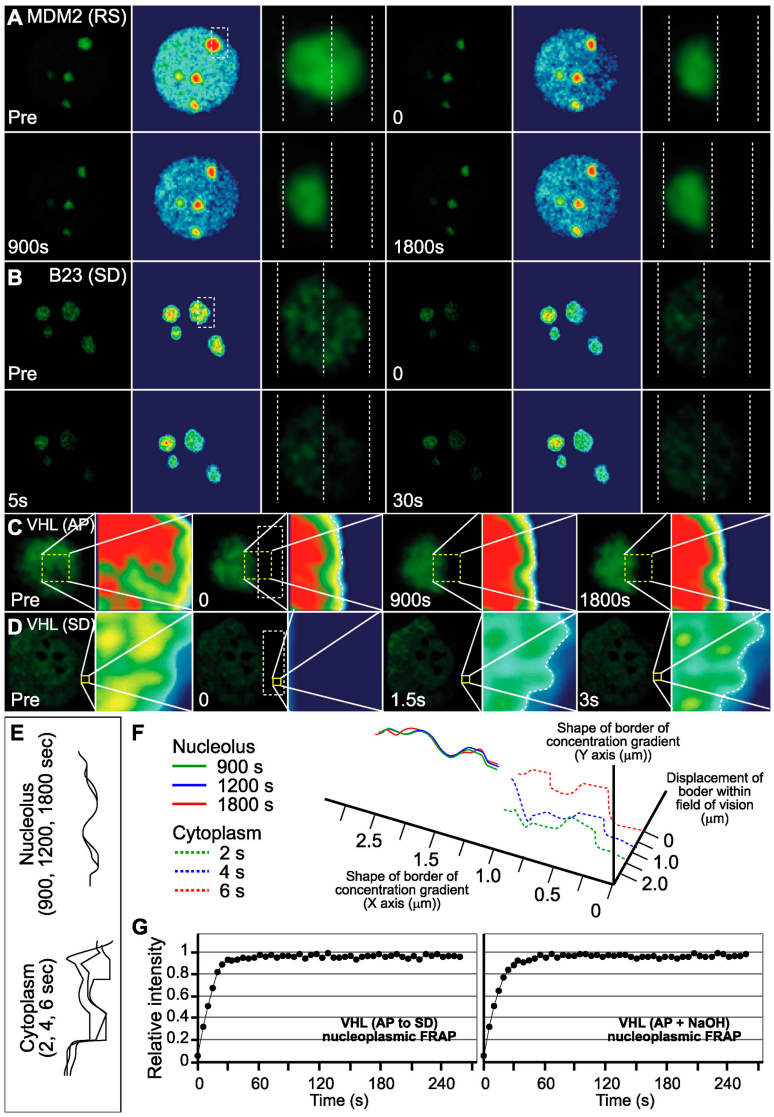

Figure 7. **Reversible static detention of VHL and MDM2 by the nucleolar architecture.** MCF7 cells were transfected to express GFP-tagged MDM2 (A), B23 (B), or VHL (C–G) and incubated under SD, AP, or RS conditions as indicated. A region representing about half of the nucleolar space (white squares) of a single nucleolus was bleached and cells were monitored by time-lapse fluorescence microscopy. Note the absence of any changes in fluorescence for nucleolar VHL and MDM2. Zoom of a single nucleolus is shown in C. Changes in the shape of the border (dashed white outline set by bleaching) of the protein concentration gradient from different time points as in C and D are overlayed in E. (F) Borders with changing (cytoplasm) or unaltered (nucleolus) shapes (plotted on X and Y axes) were monitored for their displacement away from their original position within the field of vision. Only borders set within the nucleolar space did not exhibit any movement. (G) After hypoxia-induced acidification of AP media and confinement of VHL-GFP to the nucleolus, NaOH was added to neutralize AP media (to pH 7.2) or cells were replenished with fresh SD media (pH 7.2) to induce the reversion of VHL-GFP to the nucleo-cytoplasm (also see Fig. 1). FRAP analyses in which small nucleoplasmic regions were bleached reveal that VHL-GFP resumes its high mobility profile after a return to neutral pH conditions.

Detention of ubiquitin ligases by the nucleolar architecture is a reversible process

Data presented so far suggest that the nucleolus captures the highly mobile VHL for static detention upon the establishment of cell type–specific extracellular pH threshold. We asked whether this process is reversible and if VHL can be released from nucleoli to recover its highly mobile state. VHL rapidly reverts to a diffuse nuclear cytoplasmic localization only after the reinstatement of neutral pH conditions under hypoxia or normoxia conditions (Fig. 1; Mekhail et al., 2004a). After reversion, fluorescence rapidly recovered after bleaching small nucleoplasmic regions (Fig. 7 G). These data indicate that the regulated inactivation of ligases after targeting to the nucleolus relies on their transient conversion to static participants of particular molecular networks.

Identification of a novel, discrete, pH-responsive nucleolar detention signal

Targeting of proteins to nucleoli is achieved by nucleolar localization sequence (NoLS) or nucleolar retention sequence (NoRS). These sequences are relatively large and differ considerably from nuclear import or export sequences, which are comprised of only a few amino acid residues. Therefore, we decided to identify the domain of the VBC/Cul-2 complex that mediates [H+]-regulated nucleolar sequestration of VHL. VHL is a component of the multi-protein ubiquitin ligase complex that targets the transcription factor HIF for proteasomal destruction. The complex is composed of at least VHL, elongin B, elongin C, Cullin-2, and Rbx1 (VBC/Cul-2) (Fig. 8 A; Kaelin, 2002). The ΔC157 deletion mutant of VHL, which is defective in E3 ligase complex formation (Fig. 8 A), retains the ability to target a GFP reporter to nucleoli in acidosis (Fig. 8 B, first four panels) (Pause et al., 1997; Cockman et al., 2000; Bonicalzi et al., 2001; Mekhail et al., 2004a). In contrast, Cullin-2 failed to target a GFP reporter to nucleoli of VHL-deficient cells under the same conditions (Fig. 8 B). Although these data suggest that complex formation is not required for nucleolar targeting of VHL, immunoprecipitation analysis of acidotic cells suggested that VHL can still assemble within the VBC/Cul-2 complex under acidic conditions (Fig. 8 C). Furthermore, when

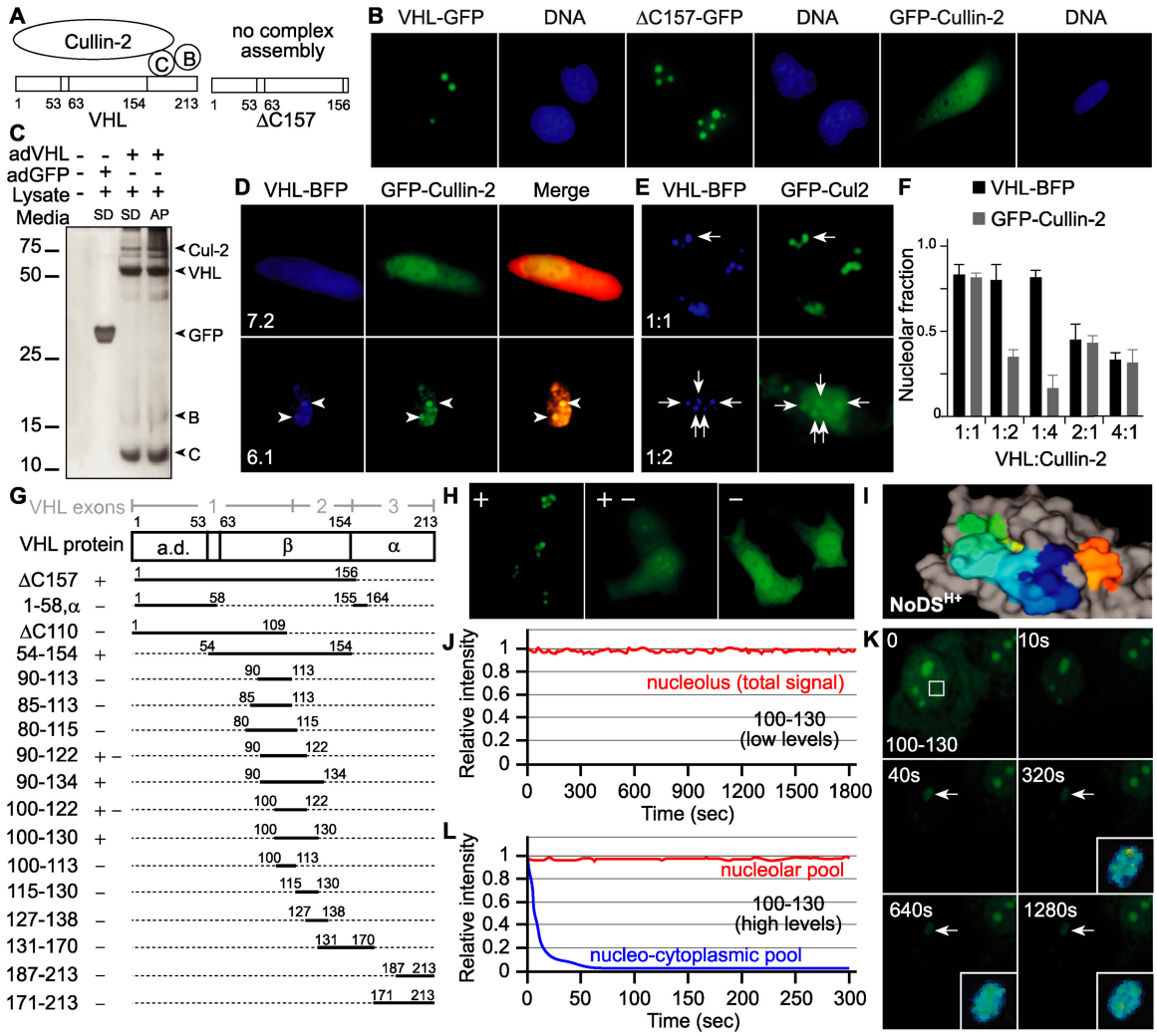

Figure 8. **pH-responsive nucleolar detention signal (NoDS^{H+}) allows VHL to target the VBC/Cul-2 ubiquitin ligase complex for static detention in the nucleolus.** (A) Schematic representation of the VBC/Cul-2 complex. ΔC157 is a mutant of VHL that fails to assemble the complex. Positions of different amino acids of VHL are indicated. (B) Complex formation is not required for nucleolar localization. VHL-deficient 786-0 cells were infected to express GFP-tagged VHL, ΔC157, or Cullin-2 and transferred to hypoxia in AP media. Acidosis triggered the nucleolar relocation of VHL-GFP and ΔC157-GFP, but not of GFP-Cullin-2. (C–F) VHL targets components of its ubiquitin ligase complex to the nucleolus. (C) VHL-deficient 786-0 cells were left uninfected or infected to express flag-tagged VHL-GFP or GFP alone and incubated in hypoxia in SD or AP media. When ∼60% of the cells in AP conditions displayed ∼30% nucleolar accumulation of VHL-GFP, cells were lysed and submitted to anti-flag immunoprecipitation and silver staining. Acidosis did not cause any sudden disruption of the VBC/Cul-2 complex. (D) VHL-deficient 786-0 cells cotransfected to transiently express VHL-BFP and GFP-Cullin-2 (1:1 ratio) were transferred to hypoxia in SD or AP conditions. Cullin-2 colocalized with VHL to the nucleolus in acidosis (arrowheads). (E and F) VHL-deficient 786-0 cells were cotransfected to transiently express VHL-BFP and GFP-Cullin-2 to varying ratios (indicated on panels and graph). VHL is the limiting factor in the nucleolar colocalization (arrows) of VHL and Cullin-2. (G) VHL mapping analysis. MCF7 cells transfected to transiently express indicated GFP-tagged proteins were incubated in AP media for 20 h in hypoxia. Schematic of *VHL* exons and derived amino acid domains are shown. Nucleolar localization was scored according to representative images in (H). Amino acid residues 100–130 of the VHL protein were identified as the minimal domain to recapitulate the nucleolar localization potential of the wild-type VHL tumor suppressor protein in acidosis. "a.d." denotes acidic domain. (I) VHL(100–130) represents a surface pocket on the VHL protein as revealed by molecular modeling (PyMOL). Each amino acid within that sequence is represented in a different color for better visualization. MCF7 cells were transfected to transiently express VHL(100–130)-GFP at low (J) or high (K and L) levels and transferred to hypoxia under AP conditions. Upon reaching a plateau for nucleolar targeting, cells were submitted to FLIP analysis in which a nucleoplasmic region (white square in K) was repeatedly bleached. Insets in K show a pseudocolored zoom of a nucleolus (arrow).

cotransfected with at least an equimolar amount of VHL, Cullin-2 colocalized with VHL in the nucleoli of acidotic cells (Fig. 8, D–F). Cullin-2 is also immobile in the nucleolus of acidic cells, suggesting that VHL responds to changes in extracellular pH and dictates the dynamic status of the assembled VBC/Cul-2 E3 ligase complex (unpublished data). Together, these data identify a novel role for the VHL tumor suppressor in regulating the subcellular trafficking dynamics of the VBC/Cul-2 ubiquitin ligase complex by targeting it to the nucleolus in response to an increase in environmental H^+ concentrations.

Mapping analyses of MDM2 and its associated proteins have previously identified small aminopeptide sequences that can target a GFP reporter protein to the nucleolus in response to various physiological signals (Weber et al., 2000; Lohrum et al., 2003). Deletion mutant analysis of VHL was therefore conducted to identify minimal nucleolar detention sequences.

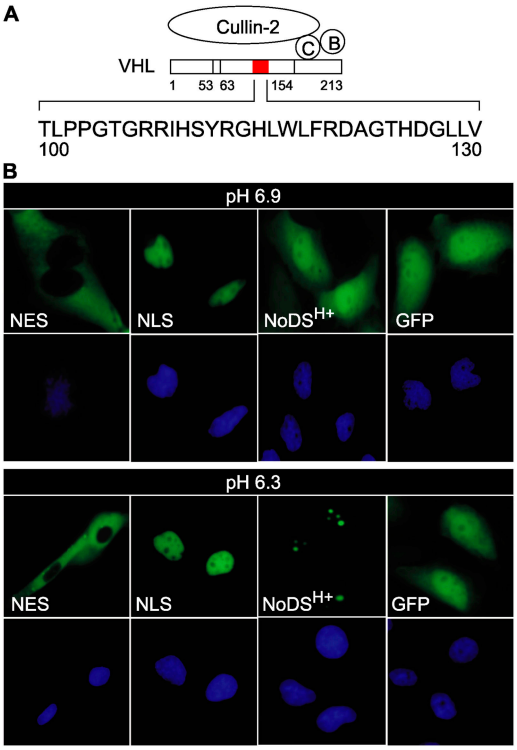

Figure 9. **Characteristics of the NoDS^{H+} sequence.** (A) Shown is a schematic representation of the VBC/Cul-2 complex. The NoDS^{H+} of VHL is highlighted in red and its constituent amino acids (residues 100–130 of VHL, inclusively) are indicated. (B) MCF7 cells were transiently transfected to express GFP-tagged NES, NLS, NoDS^{H+} or GFP alone. Cells were incubated in hypoxia under AP conditions with maximal acidifications of pH 6.9 or 6.3.

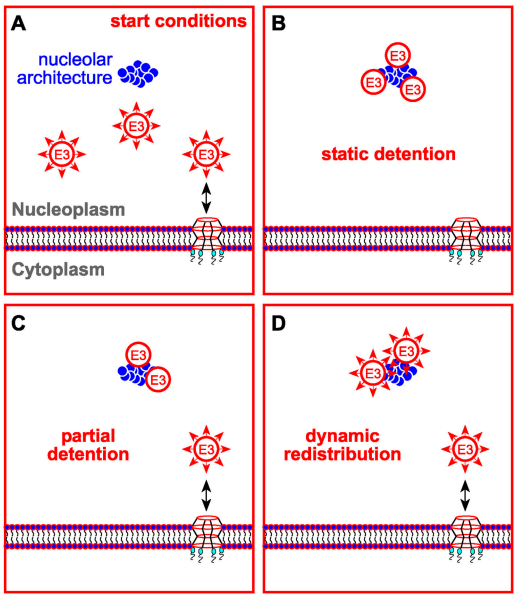

Figure 10. **Regulation of ubiquitylation networks by the nucleolus.** (A) Ubiquitin ligases follow a stochastic model of molecular mobility to ensure functional interactions such as those with the functional nuclear pore architecture at the nuclear envelope. (B) Complete static detention of ligases within the nucleolar space abolishes these required molecular interactions. (C) Detention of a fraction of the protein population results in a static nucleolar pool while a second pool sustains dynamic functions in the nucleoplasm or cytoplasm. (D) Dynamic change in the steady-state distribution of a protein from mainly nucleo-cytoplasmic to mainly nucleolar allows the protein to assume dynamic functions in the nucleolus and other cellular compartments.

Although several regions within the β-domain of VHL displayed relatively weak nucleolar localization activity in response to acidosis, a domain encoding residues 100–130 recapitulated the nucleolar targeting capability of wild-type VHL (Fig. 8, G–I). VHL(100–130) efficiently mediated the nucleolar detention of a GFP reporter in acidosis as revealed by FLIP experiments (Fig. 8 J). Neutralization of the media released VHL(100–130) into the nucleoplasm where it resumed its dynamic mobility profile (unpublished data). In addition, similar to the wild-type protein (Fig. 4, D and G), increasing the expression level of VHL(100–130) created a static nucleolar and a dynamic nucleo-cytoplasmic pool (Fig. 8, K and L). Unlike VHL(100–130), previously identified NLS and NES sequences fail to respond to increases in extracellular hydrogen ion concentrations (Fig. 9), highlighting the functional specificity of the herein identified domain. These findings identify a novel and discrete protein domain as a new type of protein localization sequence that we now refer to as [H^+]-responsive nucleolar detention signal (NoDS^{H+}).

Discussion

We provide evidence that the nucleolar architecture serves as a scaffold to convert highly mobile ubiquitin ligases to static participants of their molecular networks in response to physiological cues. This has various implications for our understanding of the role of nuclear compartments in regulating the output of dynamic molecular networks. Unlike certain core histones, which ensure chromatin stability by adopting a constitutive profile of relative immobility (Abney et al., 1997; Kimura and Cook, 2001), most proteins, including heterochromatin protein-1 (Cheutin et al., 2003; Festenstein et al., 2003; Maison and Almouzni, 2004), follow a stochastic model of high molecular mobility to ensure efficient functional interactions. We propose a model by which dynamic molecular networks, such as the ubiquitylation system, are built on complex interactions between mobile and relatively static participants. According to this model, modulation of these interactions through regulation of the dynamic state of the participants alters the output of the network. It is known that the interaction of the VBC/Cul-2 and MDM2 ubiquitin ligases with the functional nuclear pore architecture is required for nuclear export and subsequent degradation of their substrates (Fig. 10 A) (Momand et al., 1992; Oliner et al., 1993; Freedman and Levine, 1998; Roth et al., 1998; Lee et al., 1999; Groulx and Lee, 2002). Although constituents of the nuclear pore can move between subcellular compartments, functional pore architecture is confined to the nuclear envelope and persists for long periods of time within well-defined spatial regions (Rabut et al., 2004). Therefore, eliminating the physical interaction between an immobile and a mobile participant only requires the immobilization of the dynamic participant at a different spatial coordinate. In the herein described system, key interactions are abolished after static de-

tention of the ubiquitin ligases within the nucleolar space, a phenomenon that alters network output (i.e., degradation of substrates) (Fig. 10 B) as previously shown by work from our and other groups (Tao and Levine, 1999; Weber et al., 1999; Lohrum et al., 2003; Mekhail et al., 2004a). These data suggest that static nucleolar detention selectively abolishes ubiquitin ligase functions requiring interactions with immobile constituents of the ubiquitylation networks. Whether VHL or MDM2 retain other functions when sequestered in nucleoli, or assume new roles, remains unknown.

The redistribution of dynamic nucleo-cytoplasmic proteins to the nucleolus can be classified in three main categories. First, complete nucleolar detention results in the conversion of a mobile protein to a static participant of its molecular network (Fig. 10 B). Second, detention of a fraction of the protein population results in a static nucleolar pool while a second pool sustains dynamic functions in the nucleoplasm or cytoplasm (Fig. 10 C). Third, dynamic change in the steady-state distribution of a protein from mainly nucleo-cytoplasmic to mainly nucleolar allows the protein to assume dynamic functions in the nucleolus and other cellular compartments (Fig. 10 D). It is possible that a single protein can be targeted to the nucleolus through different mechanisms (Fig. 10, B–D) to custom-tailor specific dynamic profiles in response to different signals. Alternatively, ubiquitin ligases can be regulated through nonnucleolar mechanisms, such as inactivating post-translational modifications, to control ubiquitylation without altering general dynamic properties of the ligase in the cell.

Specific aminopeptide sequences, such as NLS, NES, and NoLS, target proteins to various cellular regions. Mapping analysis of the VHL tumor suppressor protein identified a new type of protein localization sequence, $NoDS^{H+}$, which is activated after a decrease in extracellular pH to target proteins for static detention in the nucleolus. $NoDS^{H+}$ is inactivated after a return to neutral pH conditions, causing rapid release of detained proteins into the nucleoplasm. The $NoDS^{H+}$ is one of the first discrete domains that have been identified to target proteins to the nucleolus and differs considerably from other NoLS and NoRS signals in its size and mode of regulation. The $NoDS^{H+}$ is characterized by the presence of several arginine residues (Fig. 9 A) that are known to be involved in targeting proteins to the nucleolus. It is possible that these residues are involved in pH-regulated targeting of VHL to nucleoli, whereas other residues play a role in static detention. Further investigation will be required to decipher the mechanisms by which extracellular hydrogen ions activate the $NoDS^{H+}$ of VHL. It will also be important to screen proteins for similar sequences, as they could play vital roles in altering general protein dynamics and metabolism in response to changes in extracellular hydrogen ion concentration. Consistent with the hypothesis that nucleolar sequestration may be a general phenomenon is the recent report that the nucleolus can capture and release several proteins in response to different cellular cues (Andersen et al., 2005).

In conclusion, our findings highlight the role of the nucleolus in regulating protein dynamics, localization, and function. We propose a model by which, via reversible interactions with the nucleolar architecture, ubiquitin ligases alternate between dynamic and static states to alter the output of their complex molecular networks. There is ample evidence that proteins are highly mobile molecules that function through stochastic interactions with binding partners. This paper provides evidence that cells have evolved a mechanism to regulate molecular networks by switching proteins between mobile and immobile states and highlight the role of the nucleolus in sequestering molecules.

Materials and methods

Cells and materials

C2C12 and PC12 cells from the American Type Culture Collection (Manassas, VA) were differentiated by lowering the serum concentration from 5 to 0.5% or by addition of NGF (50 ng ml^{-1}), respectively, before infection with adenoviruses. 786-0 (VHL-defective), U87MG, HOP62, MCF7, MDA-MB-231, SF295, and H9C2 cells were also obtained from the American Type Culture Collection. VHL-negative 117 cells were a gift from James Gnarra (Louisiana State University, Baton Rouge, LA). 786-0 (Lee et al., 1999), 117 (Mekhail et al., 2004a), or MCF7 cells stably expressing VHL–GFP were generated as described previously (Lee et al., 1999). Where indicated, fluorescein diacetate (5 μM) and propidium iodide (2 μM) (Sigma-Aldrich) were added to cells 20 min from endpoint.

Cell culture

Normoxic cells were incubated at 37°C under a 5% CO_2 environment. Hypoxia was achieved by incubation in a hypoxic chamber at 37°C under a 1% O_2, 5% CO_2, and N_2-balanced atmosphere. Acidosis (VHL) (Mekhail et al., 2004a) and ribosomal perturbation (MDM2) (Lohrum et al., 2003) experiments were conducted as previously described. For SD or AP conditions, buffer-free medium (DME; Invitrogen) was freshly prepared and supplemented with 5% (vol/vol) FBS and 1% (vol/vol) penicillin-streptomycin. $NaHCO_3$ (44 mM) was added and the pH was adjusted to 7.2 (SD) or 5.4–7.2 (AP) with HCl. Air was bubbled into both media at 22°C, which stabilizes the pH at 7.2. AP media slowly reverted to its original pH (5.4–7.2) under hypoxia, whereas the SD medium remained at pH 7.2. MDM2 ribosomal stress (RS) conditions were induced in SD media by addition of 15 nM ActD (Calbiochem) for the last 2 h of a 6-h treatment with 20 μM MG132 (Calbiochem) (Lohrum et al., 2003). Transfected or adenovirus-infected cells were grown for 24 h under standard conditions before any treatment.

Plasmids and adenoviruses

VHL and its variants and mutants were cloned between an NH_2-terminal Flag-tag and a COOH-terminal GFP-tag and into pcDNA3.1, as previously described (Bonicalzi et al., 2001; Groulx and Lee, 2002). Adenoviruses were produced using the Cre-lox recombination system. Cullin-2 construct is previously described (Groulx et al., 2000). We sincerely thank Tom Misteli (National Cancer Institute, Bethesda, MD) for providing UBF1-GFP and FIB-GFP constructs; Mark Olson (University of Mississippi Medical Center, Jackson, MS) for B23-GFP construct; Gang Pei (Shangai Institute of Biological Sciences, Shangai, China) for MDM2-GFP; and Uri Alon (Weizmann Institute of Science, Rehovot, Israel) and Galit Lahav (Harvard Medical School, Boston, MA) for MDM2-YFP. Transient transfections were conducted with Effectene transfection reagent (QIAGEN).

Immunoprecipitation

Cells lysis and immunoprecipitations were conducted as previously described (Groulx and Lee, 2002). In brief, M2 beads were added to total cell lysates containing 1 mg of protein. After 1 h tumbling at 4°C, beads were washed several times, eluted with flag peptides. Eluates were boiled before undergoing Western blotting. Gels were silver stained according to manufacturer's protocol (Bio-Rad Laboratories).

Immunoblotting

Samples were separated on denaturing polyacrylamide gels containing SDS and transferred to methanol-activated polyvinylidene difluoride membrane (NEN Life Science Products). Membranes were blocked in skimmed milk before incubation with antibodies to VHL (BD Biosciences) (Kibel et al., 1995; Corless et al., 1997; Mekhail et al., 2004a) or HIF-2α (Novus) (Mekhail et al., 2004a). After washing with a 0.2% Tween-PBS solution, membranes were blotted with a secondary antibody conjugated to HRP (Jackson ImmunoResearch Laboratories) and detected by Western Lightning Chemiluminescence Reagent Plus (PerkinElmer).

Immunofluorescence microscopy
Cells were seeded onto coverslips and fixed with prechilled (to −20°C) methanol for 10 min followed by acetone for 1 min. An anti-B23 mAb (Sigma-Aldrich) was used. Cells were incubated for 1 h with a primary antibody solution containing 10% FBS and 1% Triton X-100 (vol/vol). Cells were washed several times in PBS before 1 h incubation with a secondary Texas red–labeled antibody (Jackson ImmunoResearch Laboratories). Images of fixed cells were captured with a microscope (Axioskop 2 MOT PLUS; Carl Zeiss MicroImaging, Inc.) using a digital charged-coupled device camera (Qimaging). Compartmental fluorescence was measured as described previously (Lee et al., 1999; Mekhail et al., 2004a).

Photobleaching and microscopy
Cells cultured on 40-mm-diameter glass coverslips were visualized on a confocal microscope (MRC 1024; Bio-Rad Laboratories) in an FCS2 environmental chamber (Bioptechs) maintained at 37°C or, where indicated, directly into 35-mm dishes with coverslip bottoms. A 60× plan Apo oil immersion lens with a 1.4 NA was used for bleaching and imaging. Indicated areas were exposed to five rapid pulses of a 488-nm argon laser at 100% power and image acquisition was conducted at 1% of full laser power. For FRAP experiments, images were collected at 1- or 5-s intervals. Recovery of the fluorescent signal within a bleached region was calculated as described by Phair and Misteli (2000) following $I_{rel} = (I_{(t)}/I_{(0)}) * (T_{(0)}/T_{(t)})$, where $T_{(t)}$ is the total cellular intensity at time t, $T_{(0)}$ is total cellular intensity before bleach, $I_{(0)}$ is the intensity in the bleached area before bleach, and $I_{(t)}$ is the intensity in the previously bleached area at time t. For iFRAP nuclear export experiments the whole cytoplasm was bleached and cells were monitored in 30-s intervals. Relative loss of total fluorescence in the unbleached nucleus was calculated as $I_{rel} = (I_{(t)}/I_{(0)}) * (N_{(0)}/N_{(t)})$, where $I_{(t)}$ is the average intensity of the unbleached nucleus at time point t, $I_{(0)}$ is the average prebleach intensity of the nucleus of interest, and $N_{(0)}$ and $N_{(t)}$ are the average total cellular fluorescence intensities of a neighboring cell in the same field of vision at prebleach or at time point t, respectively. For FLIP experiments, cells were repeatedly bleached and imaged at 5-s intervals and fluorescence loss in unbleached areas was calculated similar to iFRAP calculations to account for any losses in fluorescence by normalizing the fluorescence in the cell of interest to that of a neighboring cell. Where indicated, cycloheximide (20 μg ml^{-1}) was added 1 h from endpoint. For all bleaching experiments, at least 10 datasets were analyzed for each result. Average pixel intensities were normalized for background fluorescence. Images of living cells from experiments that do not implicate bleaching were captured with a microscope (Axiovert S100TV; Carl Zeiss MicroImaging, Inc.) equipped with a 40×/1.2 C-Apochromat water immersion objective using a digital charged-coupled device camera (Empix). Pseudocoloring for bleaching and fusion experiments was achieved by applying the gradient map function of Photoshop (Adobe) to a montage of picture frames prepared with Image J (National Institutes of Health, Bethesda, MD) software. Other software packages used to capture images, analyze the data, and generate graphs include Northern Eclipse (Empix), Excel (Microsoft), and FreeHand (Macromedia).

Polykaryon assay
For VHL-GFP relocation to the nucleolus in homokaryon fusion assays, cells were transfected according to manufacturer's protocol to express fluorescent-labeled proteins and incubated under in standard conditions for 24 h (Lee et al., 1999). Usually between 40 and 60% of cells presented strong fluorescence. Cells were washed twice with warm PBS and fused for 2 min by addition of a warm 50% solution of PEG in PBS (Sigma-Aldrich). PEG was removed thoroughly by four washes with warm PBS and cells were incubated for 30 min under standard conditions. Cells were then replenished with AP media (see Cell culture) and transferred to hypoxia. After acidification, cells were monitored for the distribution of VHL-GFP in polykaryonic cells. For VHL-GFP and B23-GFP dynamic trafficking assays (Fig. 5, B and C), cells were transfected to express GFP-tagged proteins or left unaltered. The cells were then mixed at a 1:10 ratio, plated in 35-mm-diameter culture dish with a girded coverslip as its base, and exposed to hypoxia in AP media. After acidification and redistribution of VHL-GFP to nucleoli, cells were fused by PEG treatment as described above. This process yielded a significant number of polykaryonic cells where the fluorescence observed in the cell is only associated with nucleoli of only one or two nuclei, whereas other nuclei within the same polykaryonic cell displayed no fluorescence. Hypoxic cells were then rapidly washed twice with nonbuffered acidic media (pH 6.0–6.5), replenished with their original acidified AP media, and cells were monitored by fluorescence microscopy.

Online supplemental material
Fig. S1 shows characteristics of cells and VHL subcellular trafficking in hypoxia-acidosis. Fig. S2 shows that both forms of VHL relocate to the nucleolus in response to the same pH threshold in cells stably expressing the GFP-tagged proteins. Fig. S3 shows a comparison of nuclear export of VHL under neutral and acidic conditions using iFRAP. Fig. S4 shows how FLIP analysis indicates that the redistribution of MDM2 from nucleoplasm to nucleoli alters general MDM2 dynamic state. Online supplemental material available at http://www.jcb.org/cgi/content/full/jcb.200506030/DC1.

We thank Mark Olson, Tom Misteli, Gang Pei, Uri Alon, and Galit Lahav for providing plasmids. We thank Josianne Payette and Andrew Ridsdale for valuable technical support.

This work is supported by a grant from the Canadian Institutes of Health Research (CIHR). S. Lee is the recipient of the National Cancer Institute of Canada Harold E. Johns Award. K. Mekhail is supported by a Canada Graduate Scholarship (CGS-D) from the Natural Science and Engineering Research Council of Canada (NSERC).

Submitted: 6 June 2005
Accepted: 26 July 2005

References

Abney, J.R., B. Cutler, M.L. Fillbach, D. Axelrod, and B.A. Scalettar. 1997. Chromatin dynamics in interphase nuclei and its implications for nuclear structure. *J. Cell Biol.* 137:1459–1468.

Andersen, J.S., Y.W. Lam, A.K. Leung, S.E. Ong, C.E. Lyon, A.I. Lamond, and M. Mann. 2005. Nucleolar proteome dynamics. *Nature.* 433:77–83.

Appella, E., and C.W. Anderson. 2001. Post-translational modifications and activation of p53 by genotoxic stresses. *Eur. J. Biochem.* 268:2764–2772.

Azzam, R., S.L. Chen, W. Shou, A.S. Mah, G. Alexandru, K. Nasmyth, R.S. Annan, S.A. Carr, and R.J. Deshaies. 2004. Phosphorylation by cyclin B-Cdk underlies release of mitotic exit activator Cdc14 from the nucleolus. *Science.* 305:516–519.

Bonicalzi, M.E., I. Groulx, N. de Paulsen, and S. Lee. 2001. Role of exon 2-encoded beta-domain of the von Hippel-Lindau tumor suppressor protein. *J. Biol. Chem.* 276:1407–1416.

Carmo-Fonseca, M. 2002. The contribution of nuclear compartmentalization to gene regulation. *Cell.* 108:513–521.

Carmo-Fonseca, M., L. Mendes-Soares, and I. Campos. 2000. To be or not to be in the nucleolus. *Nat. Cell Biol.* 2:E107–E112.

Chen, D., and S. Huang. 2001. Nucleolar components involved in ribosome biogenesis cycle between the nucleolus and nucleoplasm in interphase cells. *J. Cell Biol.* 153:169–176.

Cheutin, T., A.J. McNairn, T. Jenuwein, D.M. Gilbert, P.B. Singh, and T. Misteli. 2003. Maintenance of stable heterochromatin domains by dynamic HP1 binding. *Science.* 299:721–725.

Ciechanover, A. 2005. Proteolysis: from the lysosome to ubiquitin and the proteasome. *Nat. Rev. Mol. Cell Biol.* 6:79–87.

Cockman, M.E., N. Masson, D.R. Mole, P. Jaakkola, G.W. Chang, S.C. Clifford, E.R. Maher, C.W. Pugh, P.J. Ratcliffe, and P.H. Maxwell. 2000. Hypoxia inducible factor-alpha binding and ubiquitylation by the von Hippel-Lindau tumor suppressor protein. *J. Biol. Chem.* 275:25733–25741.

Corless, C.L., A.S. Kibel, O. Iliopoulos, and W.G. Kaelin Jr. 1997. Immunostaining of the von Hippel-Lindau gene product in normal and neoplastic human tissues. *Hum. Pathol.* 28:459–464.

Daelemans, D., S.V. Costes, S. Lockett, and G.N. Pavlakis. 2005. Kinetic and molecular analysis of nuclear export factor CRM1 association with its cargo in vivo. *Mol. Cell. Biol.* 25:728–739.

Dundr, M., T. Misteli, and M.O. Olson. 2000. The dynamics of postmitotic reassembly of the nucleolus. *J. Cell Biol.* 150:433–446.

Dundr, M., U. Hoffmann-Rohrer, Q. Hu, I. Grummt, L.I. Rothblum, R.D. Phair, and T. Misteli. 2002. A kinetic framework for a mammalian RNA polymerase in vivo. *Science.* 298:1623–1626.

Festenstein, R., S.N. Pagakis, K. Hiragami, D. Lyon, A. Verreault, B. Sekkali, and D. Kioussis. 2003. Modulation of heterochromatin protein 1 dynamics in primary Mammalian cells. *Science.* 299:719–721.

Freedman, D.A., and A.J. Levine. 1998. Nuclear export is required for degradation of endogenous p53 by MDM2 and human papillomavirus E6. *Mol. Cell. Biol.* 18:7288–7293.

Gillette, T.G., W. Huang, S.J. Russell, S.H. Reed, S.A. Johnston, and E.C. Friedberg. 2001. The 19S complex of the proteasome regulates nucleotide excision repair in yeast. *Genes Dev.* 15:1528–1539.

Groulx, I., and S. Lee. 2002. Oxygen-dependent ubiquitination and degradation of hypoxia-inducible factor requires nuclear-cytoplasmic trafficking of the von Hippel-Lindau tumor suppressor protein. *Mol. Cell. Biol.* 22:5319–5336.

Groulx, I., M.E. Bonicalzi, and S. Lee. 2000. Ran-mediated nuclear export of the von Hippel-Lindau tumor suppressor protein occurs independently of its assembly with cullin-2. *J. Biol. Chem.* 275:8991–9000.

Kaelin, W.G., Jr. 2002. Molecular basis of the VHL hereditary cancer syndrome. *Nat. Rev. Cancer.* 2:673–682.

Kibel, A., O. Iliopoulos, J.A. DeCaprio, and W.G. Kaelin Jr. 1995. Binding of the von Hippel-Lindau tumor suppressor protein to Elongin B and C. *Science.* 269:1444–1446.

Kimura, H., and P.R. Cook. 2001. Kinetics of core histones in living human cells: little exchange of H3 and H4 and some rapid exchange of H2B. *J. Cell Biol.* 153:1341–1353.

Lam, Y.W., L. Trinkle-Mulcahy, and A.I. Lamond. 2005. The nucleolus. *J. Cell Sci.* 118:1335–1337.

Lee, S., M. Neumann, R. Stearman, R. Stauber, A. Pause, G.N. Pavlakis, and R.D. Klausner. 1999. Transcription-dependent nuclear-cytoplasmic trafficking is required for the function of the von Hippel-Lindau tumor suppressor protein. *Mol. Cell. Biol.* 19:1486–1497.

Lippincott-Schwartz, J., N. Altan-Bonnet, and G.H. Patterson. 2003. Photobleaching and photoactivation: following protein dynamics in living cells. *Nat. Cell Biol.* (Suppl):S7–S14.

Llanos, S., P.A. Clark, J. Rowe, and G. Peters. 2001. Stabilization of p53 by p14ARF without relocation of MDM2 to the nucleolus. *Nat. Cell Biol.* 3:445–452.

Lohrum, M.A., R.L. Ludwig, M.H. Kubbutat, M. Hanlon, and K.H. Vousden. 2003. Regulation of HDM2 activity by the ribosomal protein L11. *Cancer Cell.* 3:577–587.

Maison, C., and G. Almouzni. 2004. HP1 and the dynamics of heterochromatin maintenance. *Nat. Rev. Mol. Cell Biol.* 5:296–304.

Mekhail, K., L. Gunaratnam, M.E. Bonicalzi, and S. Lee. 2004a. HIF activation by pH-dependent nucleolar sequestration of VHL. *Nat. Cell Biol.* 6:642–647.

Mekhail, K., M. Khacho, L. Gunaratnam, and S. Lee. 2004b. Oxygen sensing by H+: implications for HIF and hypoxic cell memory. *Cell Cycle.* 3:1027–1029.

Michael, D., and M. Oren. 2003. The p53-Mdm2 module and the ubiquitin system. *Semin. Cancer Biol.* 13:49–58.

Misteli, T. 2001. Protein dynamics: implications for nuclear architecture and gene expression. *Science.* 291:843–847.

Momand, J., G.P. Zambetti, D.C. Olson, D. George, and A.J. Levine. 1992. The mdm-2 oncogene product forms a complex with the p53 protein and inhibits p53-mediated transactivation. *Cell.* 69:1237–1245.

Muratani, M., and W.P. Tansey. 2003. How the ubiquitin-proteasome system controls transcription. *Nat. Rev. Mol. Cell Biol.* 4:192–201.

Oliner, J.D., J.A. Pietenpol, S. Thiagalingam, J. Gyuris, K.W. Kinzler, and B. Vogelstein. 1993. Oncoprotein MDM2 conceals the activation domain of tumour suppressor p53. *Nature.* 362:857–860.

Pause, A., S. Lee, R.A. Worrell, D.Y. Chen, W.H. Burgess, W.M. Linehan, and R.D. Klausner. 1997. The von Hippel-Lindau tumor-suppressor gene product forms a stable complex with human CUL-2, a member of the Cdc53 family of proteins. *Proc. Natl. Acad. Sci. USA.* 94:2156–2161.

Paushkin, S.V., M. Patel, B.S. Furia, S.W. Peltz, and C.R. Trotta. 2004. Identification of a human endonuclease complex reveals a link between tRNA splicing and pre-mRNA 3′ end formation. *Cell.* 117:311–321.

Petroski, M.D., and R.J. Deshaies. 2005. Function and regulation of cullin-RING ubiquitin ligases. *Nat. Rev. Mol. Cell Biol.* 6:9–20.

Phair, R.D., and T. Misteli. 2000. High mobility of proteins in the mammalian cell nucleus. *Nature.* 404:604–609.

Rabut, G., V. Doye, and J. Ellenberg. 2004. Mapping the dynamic organization of the nuclear pore complex inside single living cells. *Nat. Cell Biol.* 6:1114–1121.

Roth, J., M. Dobbelstein, D.A. Freedman, T. Shenk, and A.J. Levine. 1998. Nucleo-cytoplasmic shuttling of the hdm2 oncoprotein regulates the levels of the p53 protein via a pathway used by the human immunodeficiency virus rev protein. *EMBO J.* 17:554–564.

Russell, S.J., S.H. Reed, W. Huang, E.C. Friedberg, and S.A. Johnston. 1999. The 19S regulatory complex of the proteasome functions independently of proteolysis in nucleotide excision repair. *Mol. Cell.* 3:687–695.

Semenza, G.L. 2000. HIF-1 and human disease: one highly involved factor. *Genes Dev.* 14:1983–1991.

Shou, W., J.H. Seol, A. Shevchenko, C. Baskerville, D. Moazed, Z.W. Chen, J. Jang, H. Charbonneau, and R.J. Deshaies. 1999. Exit from mitosis is triggered by Tem1-dependent release of the protein phosphatase Cdc14 from nucleolar RENT complex. *Cell.* 97:233–244.

Shou, W., K.M. Sakamoto, J. Keener, K.W. Morimoto, E.E. Traverso, R. Azzam, G.J. Hoppe, R.M. Feldman, J. DeModena, D. Moazed, et al. 2001. Net1 stimulates RNA polymerase I transcription and regulates nucleolar structure independently of controlling mitotic exit. *Mol. Cell.* 8:45–55.

Stauber, R., G.A. Gaitanaris, and G.N. Pavlakis. 1995. Analysis of trafficking of Rev and transdominant Rev proteins in living cells using green fluorescent protein fusions: transdominant Rev blocks the export of Rev from the nucleus to the cytoplasm. *Virology.* 213:439–449.

Tao, W., and A.J. Levine. 1999. P19(ARF) stabilizes p53 by blocking nucleo-cytoplasmic shuttling of Mdm2. *Proc. Natl. Acad. Sci. USA.* 96:6937–6941.

Terrell, J., S. Shih, R. Dunn, and L. Hicke. 1998. A function for monoubiquitination in the internalization of a G protein-coupled receptor. *Mol. Cell.* 1:193–202.

Tsai, R.Y., and R.D. McKay. 2005. A multistep, GTP-driven mechanism controlling the dynamic cycling of nucleostemin. *J. Cell Biol.* 168:179–184.

van den Boom, V., E. Citterio, D. Hoogstraten, A. Zotter, J.M. Egly, W.A. van Cappellen, J.H. Hoeijmakers, A.B. Houtsmuller, and W. Vermeulen. 2004. DNA damage stabilizes interaction of CSB with the transcription elongation machinery. *J. Cell Biol.* 166:27–36.

Visintin, R., E.S. Hwang, and A. Amon. 1999. Cfi1 prevents premature exit from mitosis by anchoring Cdc14 phosphatase in the nucleolus. *Nature.* 398:818–823.

Walther, R.F., C. Lamprecht, A. Ridsdale, I. Groulx, S. Lee, Y.A. Lefebvre, and R.J. Hache. 2003. Nuclear export of the glucocorticoid receptor is accelerated by cell fusion-dependent release of calreticulin. *J. Biol. Chem.* 278:37858–37864.

Weber, J.D., L.J. Taylor, M.F. Roussel, C.J. Sherr, and D. Bar-Sagi. 1999. Nucleolar Arf sequesters Mdm2 and activates p53. *Nat. Cell Biol.* 1:20–26.

Weber, J.D., M.L. Kuo, B. Bothner, E.L. DiGiammarino, R.W. Kriwacki, M.F. Roussel, and C.J. Sherr. 2000. Cooperative signals governing ARF-mdm2 interaction and nucleolar localization of the complex. *Mol. Cell. Biol.* 20:2517–2528.

Weissman, A.M. 2001. Themes and variations on ubiquitylation. *Nat. Rev. Mol. Cell Biol.* 2:169–178.